DENOISING OF ASTROPHYSICAL IMAGE MIXTURES FROM SPATIALLY VARYING NOISE

Master of Science Thesis

Sabri ÖZEN

Eskişehir, 2024

DENOISING OF ASTROPHYSICAL IMAGE MIXTURES FROM SPATIALLY VARYING NOISE

Sabri ÖZEN

Master's Thesis

Department of Electrical and Electronics Engineering

Programme in Telecommunications

Supervisor: Prof. Dr. Mehmet Tankut ÖZGEN

Eskişehir

Eskişehir Technical University

Institute of Graduate Programs

January 2024

FINAL APPROVAL FOR THESIS

This thesis titled DENOISING OF ASTROPHYSICAL IMAGE MIXTURES FROM SPATIALLY VARYING NOISE has been prepared and submitted by Sabri ÖZEN in partial fulfillment of the requirements in “Eskişehir Technical University Directive on Graduate Education and Examination” for the Degree of Master's in Electrical and Electronics Engineering Department has been examined and approved on 19/01/2024.

Committee Members		**Title, Name and Surname**	**Signature**
Member	:	Prof. Dr. Mehmet Tankut ÖZGEN	
Member	:	Prof. Dr. Temel Engin TUNCER	
Member	:	Assist. Prof. Dr. Altan ONAT	

Prof. Dr. Semra KURAMA
Director of the Institute of Graduate Programs

19/01/2024

SUPERVISOR APPROVAL

Master's student Sabri ÖZEN, whom I supervise, has completed this thesis titled DENOISING OF ASTROPHYSICAL IMAGE MIXTURES FROM SPATIALLY VARYING NOISE. According to my inspections, the work is scientifically and ethically appropriate for the student to the thesis defense exam.

Supervisor
Prof. Dr. Mehmet Tankut ÖZGEN

ABSTRACT

DENOISING OF ASTROPHYSICAL IMAGE MIXTURES FROM SPATIALLY VARYING NOISE

Sabri ÖZEN

Department of Electrical and Electronics Engineering

Programme in Telecommunications

Eskişehir Technical University, Institute of Graduate Programs, January 2024

Supervisor: Prof. Dr. Mehmet Tankut ÖZGEN

In this study, some denoising methods are compared for denoising astrophysical image mixtures from space varying noise and a graph lowpass filter based vertex-frequency graph Wiener filter is proposed for this case of space varying noise power. Performances of the methods in terms of peak signal-to-noise ratio (PSNR) are investigated on image mixtures consisting of cosmic microwave background radiation (CMB), sychrotron and galactic dust, simulated to be obtained through 70 GHz and 100 GHz microwave channels, for different mixture coefficients.

Our proposed graph Wiener filter algorithm is compared with five other prominent denoising methods; nonlocal means improved by the Sinkhorn algorithm (NLM+S), BM3D, NLGBT, OGLR and a Wiener filter algorithm in the pixel domain. Our algorithm is slightly surpassed by the NLM+S algorithm in all of tried six mixing scenarios but generally gives competitive results.

Keywords: Cosmic microwave background radiation, astrophysical images, image denoising, graph Wiener filter, spectral graph methods, graph signal processing.

ÖZET

ASTROFİZİKSEL GÖRÜNTÜ KARIŞIMLARININ KONUMLA DEĞİŞEN GÜRÜLTÜDEN ARINDIRILMASI

Sabri ÖZEN

Elektrik-Elektronik Mühendisliği Anabilim Dalı

Telekomünikasyon Bilim Dalı

Eskişehir Teknik Üniversitesi, Lisansüstü Eğitim Enstitüsü, Ocak 2024

Danışman: Prof. Dr. Mehmet Tankut ÖZGEN

Bu çalışmada, astrofiziksel görüntü karışımlarının konumla değişen gürültüden arındırılması için bazı gürültü giderme yöntemleri karşılaştırılmış ve konumla değişen gürültü gücü için alçak geçiren filtre tabanlı düğüm-sıklık çizge Wiener filtresi geliştirilmiştir. Yöntemlerin tepe sinyal-gürültü oranı (PSNR) açısından performansları, farklı karışım katsayıları için 70 GHz ve 100 GHz mikrodalga kanalları üzerinden elde edilecek şekilde simule edilmiş, kozmik mikrodalga arka plan ışınımı (CMB), senkrotron ve galaktik tozdan oluşan görüntü karışımları üzerinde araştırılmıştır.

Önerilen çizge Wiener filtre algoritmamız öne çıkan beş gürültü giderme yöntemiyle karşılaştırılmıştır; Sinkhorn algoritması ile iyileştirilmiş yerel olmayan ortalamalar yöntemi (NLM+S), BM3D, NLGBT, OGLR ve piksel alanında bir Wiener filtre algoritması. Algoritmamız, simule edilmiş altı karışım senaryosunun tümünde NLM+S algoritmasının biraz gerisinde kalmış, ancak genel olarak rekabetçi sonuçlar vermiştir.

Anahtar Sözcükler: Kozmik mikrodalga arka plan ışınımı, astrofiziksel görüntüler, gürültü giderme, çizge Wiener filtresi, spektral çizge yöntemleri, çizgesel sinyal işleme.

ACKNOWLEDGEMENTS

I thank Ercan E. Kuruoğlu and Diego Herranz for providing simulated CMB, galactic dust and synchrotron images, and noise RMS maps.

I would like to express my sincere gratitude to my advisor, Prof. Dr. Mehmet Tankut ÖZGEN, for his patience, support and sacrifices during the thesis process.

I would also like to thank Prof. Dr. Temel Engin TUNCER and Assist. Prof. Dr. Altan ONAT for serving in my committee and sharing their valuable comments.

I would like to thank my family and Ms. Merve METİNCEGİL for all their support and trust.

Sabri ÖZEN

19/01/2024

STATEMENT OF COMPLIANCE WITH ETHICAL PRINCIPLES AND RULES

I hereby truthfully declare that this thesis is an original work prepared by me; that I have behaved in accordance with the scientific ethical principles and rules throughout the stages of preparation, data collection, analysis and presentation of my work; that I have cited the sources of all the data and information that could be obtained within the scope of this study, and included these sources in the references section; and that this study has been scanned for plagiarism with “scientific plagiarism detection program” used by Eskişehir Technical University, and that “it does not have any plagiarism” whatsoever. I also declare that, if a case contrary to my declaration is detected in my work at any time, I hereby express my consent to all the ethical and legal consequences that are involved.

Sabri ÖZEN

CONTENTS

Page

LIST OF TABLES

Page

LIST OF FIGURES

GLOSSARY OF SYMBOLS AND ABBREVIATIONS

NLM + S	:	Non-Local Means Improved by the Sinkhorn Algorithm
BM3D	:	Block-Matching and Three-Dimensional Filtering
NLGBT	:	Non-Local Graph-based Algorithm
OGLR	:	Optimal Graph Laplacian Regularization Method
SPW	:	Local Spatial Wiener Filter
LPF-VFW	:	Lowpass Filter Based Vertex-Frequency Wiener Filter
CMB	:	Cosmic Microwave Background Radiation
PSNR	:	Peak Signal-to-Noise Ratio
MSE	:	Mean Square Error
GFT	:	Graph Fourier Transform
cGRD	:	Cross Graph Rihaczek Vertex-Frequency Signal Distribution
RMS	:	Root Mean Square
$x(n)$	:	Original graph signal
$\bar{x}(n)$	:	Normalized version of $x(n)$
$y(n)$	:	Noisy graph signal
$\mathcal{L}$	:	Graph Laplacian matrix
$V=[V(n,\lambda_l)]$	:	Eigenvector matrix of the graph Laplacian $\mathcal{L}$ nth element of the eigenvector of $\mathcal{L}$ corresponding to lth eigenvalue λ_l
$V^{-\circ}=[1/V(n,\lambda_l))]$	:	A matrix formed by inverses of graph basis elements, assuming that they are nonzero
$h(n,m)$	:	Vertex-domain impulse response elements
$\mathcal{H}_{wiener}(n,\lambda_l)$	:	Vertex-frequency Wiener transfer function elements

1. INTRODUCTION

Astrophysical image mixtures consist of various components including cosmic microwave background (CMB) radiation, galactic dust and synchrotron radiation, among others [1, 2]. They are corrupted by nonstationary instrumental noise modeled as zero-mean, additive, white Gaussian noise with spatially varying variance [3]–[7].

To denoise astrophysical image mixtures from this nonstationary noise, in this work, we first propose a spectral graph based vertex-frequency graph Wiener filter for denoising of generic graph signals defined on weighted and undirected graphs from nonstationary noise with vertex varying variance. A vertex-frequency graph Wiener filter for image and graph signal denoising has already been developed for fixed noise power [8]. This thesis extends that approach to derive a vertex-frequency graph Wiener filter for the vertex varying noise power case. In this thesis our aim is to denoise image mixtures instead of obtaining the CMB component only. Spatially varying noise variances are already known in this application; therefore, we do not have the estimate noise variances in our work.

To develop a practical Wiener filter algorithm for denoising of noisy image mixtures, we assume that an original, noiseless image mixture can be regarded as a deterministic graph signal over a regular two-dimensional (2-D) grid graph, where each image pixel corresponds to a graph node. We model the relationships between pixels using graph weights. Therefore, the eigenvectors of the obtained graph Laplacians are specifically selected for the images. Then, we propose a graph lowpass filter based denoising algorithm to estimate the derived graph Wiener transfer function for this deterministic original signal assumption, from a single realization of the input, noisy image mixture to subsequently apply it to the noisy input for denoising in the vertex-frequency domain.

Denoising of additive Gaussian nonstationary noise with varying power has been previously performed by local Wiener filtering techniques in the pixel domain [9]–[11]. A denoising convolutional neural network has also been developed for space varying noise in [12]. Denoising methods for astronomical images are reviewed in [13].

Graph signal processing has been developed for signals defined or sensed on irregular domains [14, 15]. In particular, spectral graph methods rely on definition of a graph Fourier transform (GFT) [14]–[18]. Filtering in GFT domain has been proposed to process graph signals [14]–[20]. GFT domain filtering has been used for image and graph signal denoising [19, 21]. Lowpass filtering in GFT domain [14, 16, 17, 20], [22]–[28], soft thresholding [16, 17] and hard thresholding [29]–[31] of the GFT coefficients of a noisy graph signal or image are basic spectral graph based denoising methods.

Stationary graph Wiener filters to minimize the mean square error (MSE) between original and reconstructed signals while denoising or deconvolving stationary graph signals have been the next step [20], [32]–[34], [35]. But, if a graph signal or image to be reconstructed is nonstationary or deterministic, the Wiener filter takes a vertex varying or vertex-frequency form.

Denoising in the graph wavelet transform domain by thresholding noisy transform coefficients [36]–[39] can be considered as a form of vertex-frequency filtering. A vertex-frequency graph Wiener filter for removal of noise with fixed power has been previously developed for the case of deterministic original, noiseless signal or image [8]. In this thesis, we develop such a vertex- frequency graph Wiener filter to clean nonstationary noise with vertex varying noise power, and then use it to denoise astrophysical image mixtures from the nonstationary instrumental noise.

The organization of this thesis is given below. Background information on astrophysical images and graph signal processing basics, together with the graph signal model for the considered denoising problem are provided in Chapter 2. Under the assumption of a deterministic original signal, we derive the Wiener vertex-frequency transfer function in terms of the cross graph Rihaczek vertex-frequency signal distribution (cGRD) [8] of the original, noiseless graph signal and its variance-normalized version, in Chapter 3. In Chapter 4, we propose our graph Wiener denoising algorithm that estimates the Wiener transfer function from the pre-denoised output of a preliminary graph lowpass filter. In this algorithm, eigenbases of graph Laplacian matrices constructed from Gaussian prefiltered versions of noisy image mixture vectors are used as graph bases, when computing the GFT of the lowpass filter output.

In Chapter 5, to obtain a set of benchmarks for denoising of astrophysical image mixtures simulated to be received through 100 GHz and 70 GHz microwave channels with different mixing coefficients, we compute the Wiener vertex-frequency transfer function by using the original, noiseless image mixture vectors instead of the noisy ones, and graph bases similar to those of the proposed algorithm. We apply these more idealistic Wiener filters to noisy image mixtures, for three mixing coefficient scenarios for each channel. Resulting peak signal-to-noise ratio (PSNR) values can be regarded as a set of benchmarks to compare performances of practical denoising algorithms for this application. Obtained very high PSNR values also justify the assumption of deterministic original signal used to derive the proposed Wiener filter.

Proposed graph Wiener algorithm is compared with the local spatial Wiener filter [10] (SPW), the nonlocal means filter [40]–[42] improved by the Sinkhorn algorithm [43] (NLM+S), the BM3D algorithm [44, 45], and two graph based denoising methods, NLGBT [29] and OGLR [25] algorithms, in Chapter 6. Achieved PSNR values of these six algorithms are compared for three simulated mixtures, for each of 100 GHz and 70 GHz channels. These astrophysical image mixtures are also sensed through various other microwave channels, but mixture coefficients simulating 100 GHz and 70 GHz channels are available to us only. Chapter 7 summarizes and concludes the thesis.

2. BACKGROUND

2.1. Astrophysical Image Mixtures

In this work, we aim to denoise astrophysical image mixtures containing three components; CMB, galactic dust and synchrotron radiation maps, corrupted by nonstationary instrumental noise. These image components are normalized temperature measurements viewed as 2-D functions of discrete angular variables of the spherical coordinate system [1, 2, 46]. CMB is the most important component among them. It is the relic of early radiation released about 379,000 years after the Big Bang, and thus yields a picture of the early Universe [1, 2]. Galactic dust consists of very small particles [2]. Synchrotron radiation is the electromagnetic radiation generated by electrons spiraling throughout magnetic fields [2].

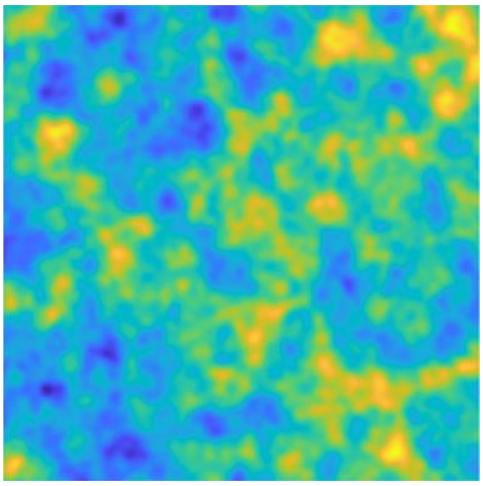

Figure 2.1. *Simulated CMB image*

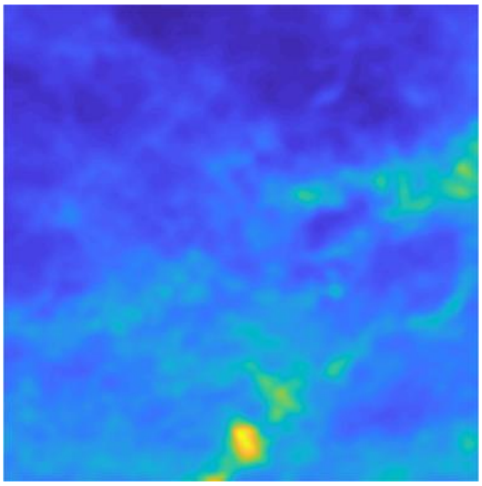

Figure 2.2. *Simulated galactic dust image*

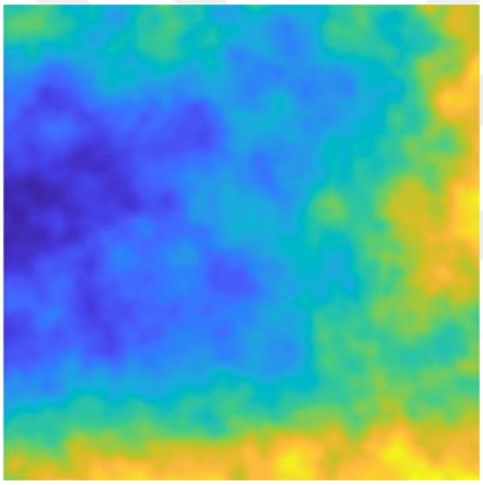

Figure 2.3. *Simulated synchrotron image*

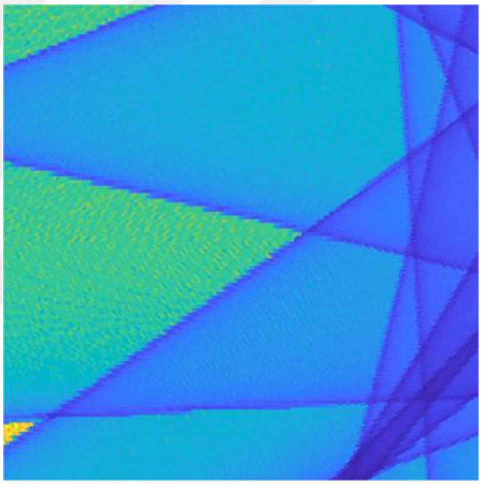

Figure 2.4. *100 GHz noise RMS map*

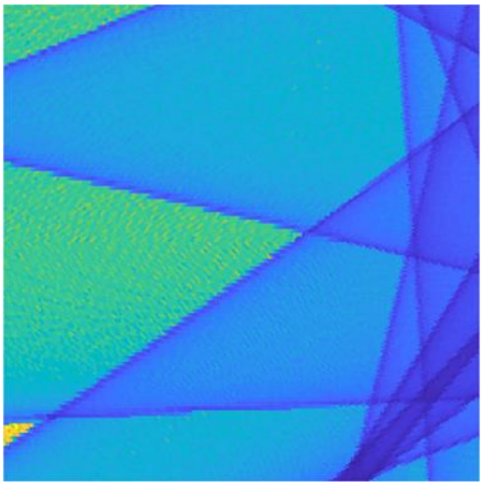

Figure 2.5. *70 GHz noise RMS map*

Figs. 2.1, 2.2 and 2.3 display simulated CMB, galactic dust and synchrotron sky maps, respectively, corresponding to 12.8 × 12.8 square degree region of the sky located 45 degrees above the Galactic plane [4, 46]. Axes of these 256 × 256 images correspond to spherical angular coordinates. Each pixel value gives the difference between the temperature in Kelvin sensed in that direction and the average temperature over all directions, divided by the average temperature. The signal root-mean-square (RMS) values of these simulated CMB, dust and synchrotron images are on the order of 10^{-5}, 10^{-6}, and 10^{-7} [4, 46].

Mixtures of these three image components simulated to be received through 100 GHz and 70 GHz channels are modeled with corresponding mixing coefficients, in Chapter 6. Then, zero- mean, additive, white Gaussian noise with space varying variance is added to them, to simulate nonstationary instrumental noise. Noise RMS maps that carry standard deviation values of noise samples pixelwise are shown for 100 GHz and 70 GHz channels in Figs. 2.4 and 2.5, respectively. Mean standard deviations are 7.92×10^{-6} and 2.19×10^{-5} for 100 GHz and 70 GHz channels, respectively [4, 46].

Simulated CMB image and noise RMS maps are provided by the Instituto de Fisica de Cantabria (IFCA). Simulated galactic dust and synchrotron images are taken from 2006 version of the Planck Reference Sky Model prepared by Planck Working Group 2 [46].

2.2. Graph Signal Processing Fundamentals

Images can be considered as signals defined on an undirected, weighted and connected graph $G = \{V, E, W\}$ [47]. This graph consists of a set of vertices V which represents pixels, a set of edges between vertices E and a weighted adjacency matrix W. If vertices i and j are connected to each other by an edge $e = (i, j)$, then w_{ij} represents the positive weight of edge.

$$w_{ij} = \begin{cases} w_e & (if\ e\ connects\ vertices\ i\ and\ j) \\ 0 & (otherwise) \end{cases} \tag{2.1}$$

Since we consider images as undirected graphs, W is a real symmetric matrix.

Graph Laplacian is defined as $\mathcal{L} = D - W$ [14, 48], where D is the diagonal degree matrix containing row sums of the matrix W [14]. Because the graph Laplacian $\mathcal{L}$ is a real symmetric matrix, it admits the eigendecomposition $\mathcal{L} = VSV^T$ such that $VV^T = V^T = I$.

V is the eigenvector matrix that takes eigenvectors as columns and S is the eigenvalue matrix. The eigenvalue matrix $S = diag(\lambda_0, \lambda_2, \dots, \lambda_{N-1})$ consists of real eigenvalues (sorted in increasing order) of the graph Laplacian along the diagonal.

Signal measurement model is given by $\underline{y} = \underline{x} + \underline{w}$ where $\underline{y}$ is column stacked noisy graph signal vector and $\underline{w}$ is the zero-mean, white Gaussian noise vector of dimension L. In our application $\underline{y}$ is obtained by stacking columns of a noisy image mixture. We assume that $\underline{w}$ contains independent, zero-mean Gaussian noise samples with space varying variance $\sigma^2(n)$. E denotes the statistical expectation operation below.

$$E\{\, w(m)\, w(n)\} = \sigma^2(n)\delta(m-n) \tag{2.2}$$

$$E\{w(m)\, w(n)\} = 0\,, \qquad m \neq n$$

$$E\{w^2(n)\} = \sigma^2(n), \qquad n = 1,2,\dots,L$$

The graph Fourier transform of $\underline{y}$ is defined as $\underline{y_f} = V^T \underline{y}$, yielding GFT coefficients as

$$y_f(\lambda_l) = \sum_{n=1}^{L} V(n,\lambda_l) y(n), \qquad l = 0,1,\dots,L-1.$$

The graph signal $\underline{y}$, is then obtained back by inverse GFT as follows,

$$y(n) = \sum_{l=0}^{L-1} V(n,\lambda_l)\, y_f(\lambda_l), \qquad n = 1,2,\dots,L.$$

3. VERTEX-FREQUENCY GRAPH WIENER FILTER FOR NONSTATIONARY NOISE

The estimate $\underline{\hat{x}}$, of an original, noiseless graph signal $\underline{x}$, can be defined as $\underline{\hat{x}} = H\underline{y}$, where $H = [h(n,m)]_{L\,x\,L}$ is the impulse response matrix, so as to minimize

$$MSE = \frac{1}{L}E\left\{\left\|\underline{x} - H\underline{y}\right\|^2\right\}. \tag{3.1}$$

When MSE is minimized, error is orthogonal to data

$$e(n) = x(n) - \hat{x}(n) = x(n) - \sum_{m=1}^{L} h(n,m)y(m) \perp y(l), \quad l = 1,2,\dots,L \tag{3.2}$$

Since the dot product is zero due to orthogonality, the statistical expectation of their product is also zero :

$$E\{e(n)y(l)\} = 0\,, \qquad n = 1,2,\dots,L, \qquad l = 1,2,\dots,L \tag{3.3}$$

When $e(n)$ is substituted into Eq. (3.3), the following equation is obtained :

$$\sum_{m=1}^{L} h(n,m)\,E\{y(m)y(l)\} = E\{x(n)y(l)\}\,, \quad n = 1,2,\dots,L, \qquad l = 1,2,\dots,L \tag{3.4}$$

Impulse response matrix of the Wiener filter can be obtained from Eq. (3.4) as follows. Using Eq. (2.2) and the signal measurement model, and Λ denoting $diag(\sigma^2(1), \sigma^2(2), \dots, \sigma^2(L))$;

$$H_{wiener} = \underline{x}\,\underline{x}^T[\Lambda + \underline{x}\,\underline{x}^T]^{-1}\,, \tag{3.5}$$

assuming that the noiseless graph signal $\underline{x}$ is deterministic. Thus, graph Wiener filter elements in vertex domain , $h_{wiener}(m,n)$'s , are obtained as follows by applying Sherman-Morrison-Woodbury formula to the matrix above :

$$h_{wiener}(m,n) = \frac{x(m)\bar{x}(n)}{1 + \sum_{n=1}^{L}\frac{x^2(n)}{\sigma^2(n)}}\,, \quad m = 1,2,\dots,L, \qquad n = 1,2,\dots,L, \tag{3.6}$$

where a normalized signal $\bar{x}(n)$ is defined as

$$\bar{x}(n) \triangleq \frac{x(n)}{\sigma^2(n)} . \tag{3.7}$$

The matrix form of Eq. (3.6) is given as

$$H_{wiener} = [h_{wiener}(m,n)] = \frac{\underline{x}\,\underline{\bar{x}}^T}{1+\ \underline{x}^T \Lambda^{-1} \underline{x}} \tag{3.8}$$

where $\underline{\bar{x}}$ is the normalized signal vector.

The graph transfer function matrix can be obtained by using the transformation given by Eq. (13) in [8] ;

$$\mathcal{H} = (HV) \circ V^{-\circ} \tag{3.9}$$

where $\circ$ denotes elementwise (Hadamard) product of matrices, and $V^{-\circ} \triangleq [1/V(n,\lambda_l)]_{L\,x\,L}$.

Substituting Eq. (3.8) into Eq. (3.9), and using $\underline{\bar{x}}_f = V^T \underline{\bar{x}}$ as the graph Fourier transform (GFT) of the normalized signal vector $\underline{\bar{x}}$, graph Wiener transfer function matrix can be obtained as follows :

$$\mathcal{H}_{wiener} = \frac{\underline{x}\,\underline{\bar{x}}_f^{\ T}}{1+\ \underline{x}^T \Lambda^{-1} \underline{x}} \circ V^{-\circ} . \tag{3.10}$$

Thus, graph Wiener filter transfer function can be written as

$$\mathcal{H}_{wiener}(n,\lambda_l) = \frac{x(n)\, \bar{x}_f(\lambda_l)\, V(n,\lambda_l)}{V^2(n,\lambda_l)[1+\sum_{n=1}^{L} \frac{x^2(n)}{\sigma^2(n)}]} \ ,$$
$$n = 1,2,\dots,L\,, \qquad l = 0,1,\dots,L-1\,. \tag{3.11}$$

From Sec. V of [8] , the cross graph Rihaczek distribution (cGRD) of graph signals $x(n)$ and $\bar{x}(n)$ are given by,

$$R_{x\bar{x}}(n,\lambda_l) = x(n)\, \bar{x}_f(\lambda_l)\, V(n,\lambda_l). \tag{3.12}$$

When Eq. (3.12) is substituted into Eq. (3.11), graph Wiener filter transfer function can be obtained as follows :

$$\mathcal{H}_{wiener}(n,\lambda_l) = \frac{R_{x\bar{x}}(n,\lambda_l)}{V^2(n,\lambda_l)[1+\sum_{n=1}^{L} \frac{x^2(n)}{\sigma^2(n)}]} \,,$$
$$n = 1,2,\dots,L\,, \qquad l = 0,1,\dots,L-1\,. \tag{3.13}$$

4. PROPOSED GRAPH WIENER ALGORITHM

The graph basis matrix V is obtained as follows, to stabilize it against noise effects. The noisy image vector $\underline{y}$ is first passed through a Gaussian pre-filter. Adjacency matrix elements are computed from the output image vector of the Gaussian filter ;

$$W_{ij} = \exp\left(\frac{-\left(\tilde{x}_i - \tilde{x}_j\right)^2}{h_x^2}\right), \tag{4.1}$$

for $i, j = 1,2, \ldots, L$, where $\tilde{x}_i$ and $\tilde{x}_j$ are i_{th} and j_{th} elements of the output image vector. h_x is a smoothing parameter in the image domain. Then, the graph Laplacian $\mathcal{L}$ is derived from this adjacency matrix with elements given by Eq. (4.1). The eigenvector matrix of this graph Laplacian is taken as the graph basis matrix V used in our algorithm. The GFT of the noisy image vector is computed as $\underline{y_f} = V^T \underline{y}$.

Since the original noiseless image vector $\underline{x}$ is not available, the proposed Wiener transfer function can be estimated by first passing the noisy input image vector through a preliminary graph lowpass filter and using its output.

The GFT of the output of this preliminary graph lowpass filter (LPF) is given by,

$$x_{f,LPF}(\lambda_l) = \frac{1}{1+\alpha\lambda_l} y_f(\lambda_l) \quad l = 0,1, \ldots, L-1 , \tag{4.2}$$

where $\underline{y_f}$ is GFT of the noisy input image to be denoised and α is a positive parameter to be searched for best performance.

The output signal of graph LPF $\underline{x}_{LPF}$, can be obtained by taking the inverse GFT as,

$$\underline{x}_{LPF} = V \, \underline{x}_{f,LPF}$$

Using Eq. (3.7) , the normalized graph LPF output signal $\underline{\overline{x}}_{LPF}$, can be written as follows,

$$\overline{x}_{LPF}(n) = \frac{x_{LPF}(n)}{\sigma^2(n)}$$

The GFT of the normalized LPF output signal $\underline{\overline{x}}_{f,LPF}$, can be obtained by,

$$\underline{\overline{x}}_{f,LPF} = V^T \, \underline{\overline{x}}_{LPF}$$

From Sec. V of [8] , the cGRD of graph signals $x_{LPF}(n)$ and $\overline{x}_{LPF}(n)$ is given by,

$$R_{x_{LPF},\ \overline{x}_{f,LPF}}(n,\lambda_l) = x_{LPF}(n)\ \overline{x}_{f,LPF}(\lambda_l)\ V(n,\lambda_l),$$
$$n = 1,2,\dots,L\,, \qquad l = 0,1,\dots,L-1\,. \tag{4.3}$$

Then the estimated Wiener transfer function is obtained from (3.13), by omitting the constant term in the denominator as,

$$\mathcal{H}_{wien,est}(n,\lambda_l) = \frac{R_{x_{LPF},\ \overline{x}_{f,LPF}}(n,\lambda_l)}{V^2(n,\lambda_l)} \tag{4.4}$$

Since dividing by $V^2(n,\lambda_l)$ terms in the denominator of Eq. (4.4) may result in division by very small terms, upper bound and lower bound values, U and L , must be determined to limit magnitude values of the transfer function. These upper bound and lower bound values are considered as design parameters and they should be searched for each image patch to achieve the best performance.

$$\mathcal{H}_{wien,est}(n,\lambda_l) = \max\left\{\min\left[\frac{R_{x_{LPF},\ \overline{x}_{f,LPF}}(n,\lambda_l)}{V^2(n,\lambda_l)}\ ,U\right],L\right\} \tag{4.5}$$

The unscaled output signal $\underline{\hat{x}}_{unscaled}$, is obtained from the output of the filter in Eq. (4.5) , as follows :

$$\hat{x}_{unscaled}(n) = \sum_{l=0}^{L-1} V(n,\lambda_l)\ \mathcal{H}_{wien,est}(n,\lambda_l)\ y_f(\lambda_l)\,, \quad n = 1,2,\dots,L \tag{4.6}$$

The scaling factor omitted in the denominator in Eq. (4.4), $1+\sum_{n=1}^{L}\frac{x^2(n)}{\sigma^2(n)}$, is taken into account by using sample means of the noisy signal $\underline{y}$ and the unscaled output signal $\underline{\hat{x}}_{unscaled}$, since mean$(\underline{y})\ \approx\ $mean$(\underline{x})$ for zero mean noise. Thus, the denoised signal $\underline{\hat{x}}_{wien}$ is obtained as,

$$\underline{\hat{x}}_{wien} = \frac{mean\left(\underline{y}\right)}{mean\left(\underline{\hat{x}}_{unscaled}\right)}\left(\underline{\hat{x}}_{unscaled}\right). \tag{4.7}$$

To improve our result, we add a second step in our algorithm as follows. We pass the output of the first step given by Eq. (4.7) through a second graph lowpass filter, similarly to Eq. (4.2). The parameter of this second lowpass filter is also a design parameter to be searched for best performance. From the output of this second lowpass filter, we calculate an improved estimate of the cGRD, similarly to Eq. (4.3). From this improved estimate, we then compute an improved Wiener transfer function, similarly to Eq. (4.5). Upper and lower bounds, U and L, of this new transfer function estimate are additional design parameters. This new transfer function estimate is applied to the output image vector of the first step, similarly to Eqs. (4.6) and (4.7).

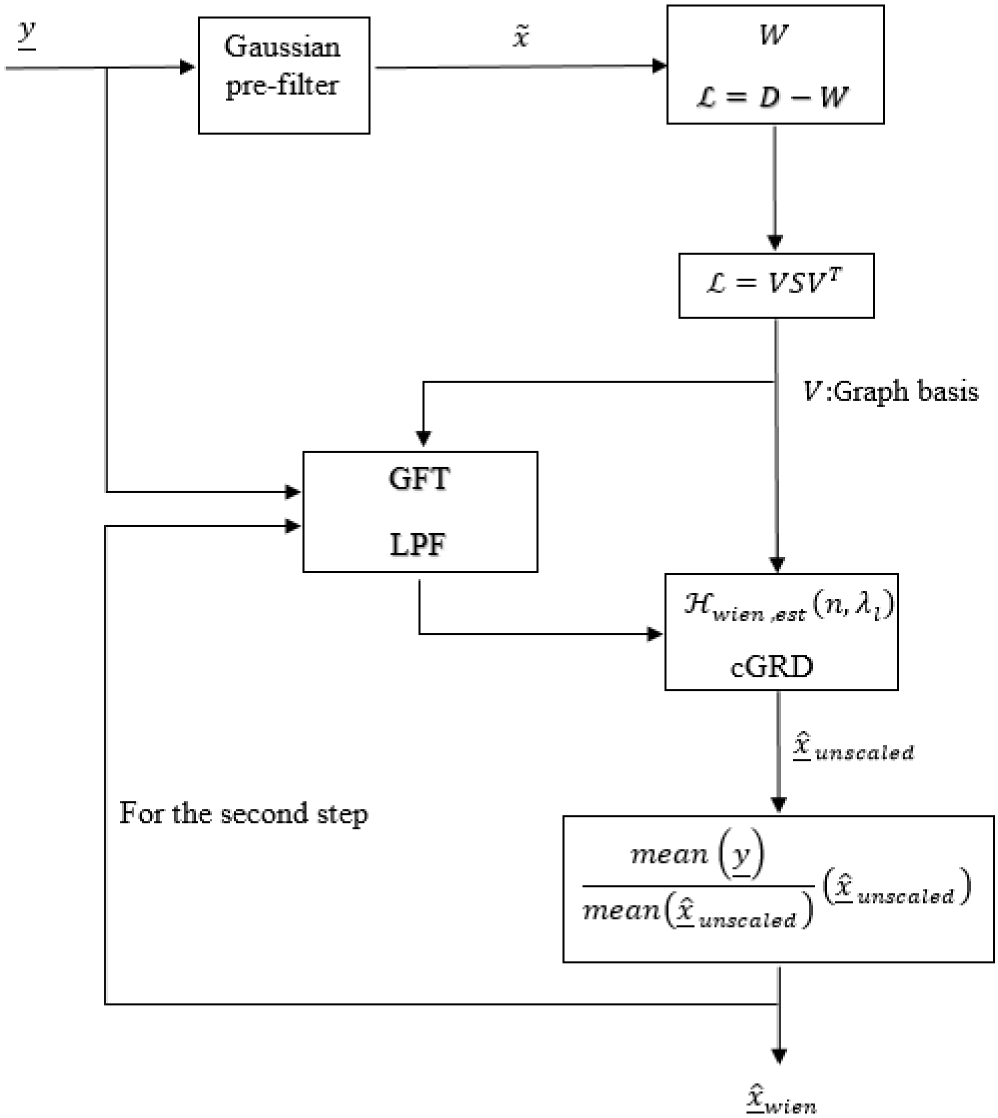

Figure 4.1. *Flowchart demonstrating the proposed denoising method*

5. BENCHMARKS

Under the assumption of noiseless graph signal $\underline{x}$ being deterministic and available, the cGRD of graph signals $x(n)$ and $\bar{x}(n)$ is calculated similarly to Eq. (4.3). With the obtained cGRD, the ideal Wiener transfer function is derived similarly to that in Eq. (4.5), as also shown below.

$$\mathcal{H}_{wien\,,ideal}(n,\lambda_l) = max\left\{min\left[\frac{R_{x\,,\,\bar{x}}(n,\lambda_l)}{V^2(n,\lambda_l)}\,,U\right],L\right\}$$

The design parameters U and L are used again to limit the magnitude values of this ideal Wiener transfer function above. The unscaled output signal is obtained from the output of this ideal Wiener filter transfer function applied to the noisy input image, similarly to Eq. (4.6). Then, denoised signal is obtained by dividing this unscaled output signal by the constant term previously omitted from the denominator in Eq. (4.4).

The obtained MSE values as above are then converted to peak-signal-to-noise ratio (PSNR) values, as follows:

$$PSNR = 10log_{10}\left(\frac{[\max(\underline{x})]^2}{MSE}\right). \tag{5.1}$$

These PSNR values obtained for six mixing coefficient cases for 100 GHz and 70 GHz channels constitute our set of benchmarks, for the considered astrophysical image mixture denoising application.

6. EXPERIMENTAL RESULTS

In this work, we apply LPF-VFW (Lowpass filter based Vertex-Frequency Wiener filter) algorithm presented in Chapter 4 and NLM+S, NLGBT, BM3D, OGLR, SPW algorithms for denoising astrophysical image mixtures simulated to be recieved from 100 GHz and 70 GHz channels. These image mixtures are modeled by different mixing coefficients. For the 100 GHz channel mixture, CMB coefficient is c_1 = 1, dust coefficient is c_2 = 1 and synchrotron coefficient is c_3 = 1. We simulated three different galactic contaminations by multiplying the components by certain numerical factors, in addition to the above coefficients. These component factors are n_d = 1, 100, 1000 for dust and n_s = 1, 100, 200 for synchrotron.

$$M[100\ GHz] = c_1 \times CMB + n_d \times c_2 \times Dust + n_s \times c_3 \times Synchrotron$$

For the 70 GHz channel mixture, CMB coefficient is c_1 = 1, dust coefficient is c_2 = 0.5085 and synchrotron coefficient is c_3 = 2.7101. We simulated three different galactic contaminations by again multiplying the components with specific numerical factors, similar to the image mixtures at 100 GHz ; n_d = 1, 100, 1000 for dust and n_s = 1, 100, 200 for synchrotron.

$$M[70\ GHz] = c_1 \times CMB + n_d \times c_2 \times Dust + n_s \times c_3 \times Synchrotron$$

100 GHz and 70 GHz noise RMS maps given in Figs. 2.4 and 2.5, respectively, are scaled so that mean noise standard deviations for 100 GHz and 70 GHz channels are set to 7.92×10^{-6} and 2.19×10^{-5}, respectively.

Then, Gaussian noise samples with zero-mean and unity variance are multiplied by scaled RMS values and added to noiseless image mixtures, pixelwise, to obtain noisy mixtures with nonstationary noise with space varying variance.

Our proposed algorithm LPF-VFW and the NLM+S method are used patchwise. They are applied to each one of the 16 64 × 64 patch of a 256 × 256 noisy image mixture, because of their computational cost. Their optimal parameters are found for each patch, separately. Other algorithms are applied to entire 256 × 256 noisy images.

Table 6.1. *PSNR values (in dB) for LPF-VFW, NLM + S, NLGBT, BM3D, OGLR, SPW and Ideal Wiener Filter algorithms. PSNR results are obtained from MSE results averaged over 15 independent noise realizations.*

	100 GHz Dust : 1 Synchrotron : 1	**100 GHz Dust : 100 Synchrotron : 100**	**100 GHz Dust : 1000 Synchrotron : 200**	**70 GHz Dust : 1 Synchrotron : 1**	**70 GHz Dust : 100 Synchrotron : 100**	**70 GHz Dust : 1000 Synchrotron : 200**
LPF-VFW	31.6138	45.2512	59.5531	26.3470	35.7113	49.6021
NLM+S	32.6272	45.9934	59.8909	26.9493	36.4395	50.1991
NLGBT	32.2413	46.5856	62.9624	25.3245	35.3406	50.7187
BM3D	31.3392	45.2740	61.3423	25.1277	34.8813	49.9055
OGLR	30.7406	44.5233	58.3778	23.1502	33.3178	48.1887
SPW	28.9938	42.7292	59.1317	22.4879	32.0703	47.1197
Ideal Wiener Filter	59.1327	73.5482	82.7287	50.6823	61.2528	75.6851

In Table 6.1, the denoising accuracies of LPF-VFW, NLM+S, NLGBT, BM3D, OGLR, SPW algorithms and the ideal Wiener filter are given for six image mixtures. The denoised outputs of our proposed Wiener filter (LPF - VFW) and the NLM + S algorithm, which gives the highest accuracy for n_d = 1, n_s = 1 factors, for 100 GHz and 70 GHz channels, are given in the figures below.

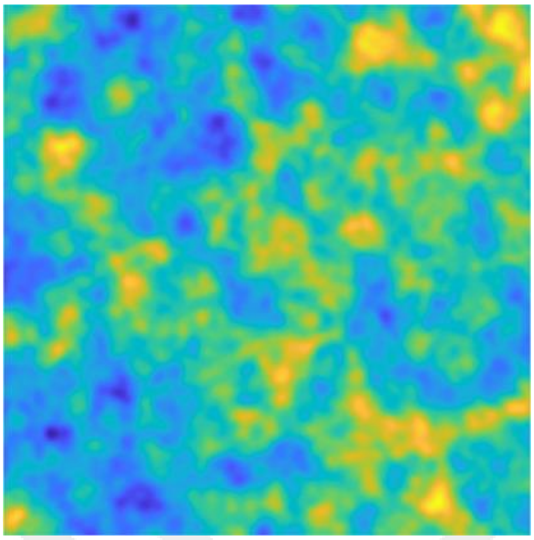

Figure 6.1. *Noiseless image for 100 GHz, nd = 1, ns =1.*

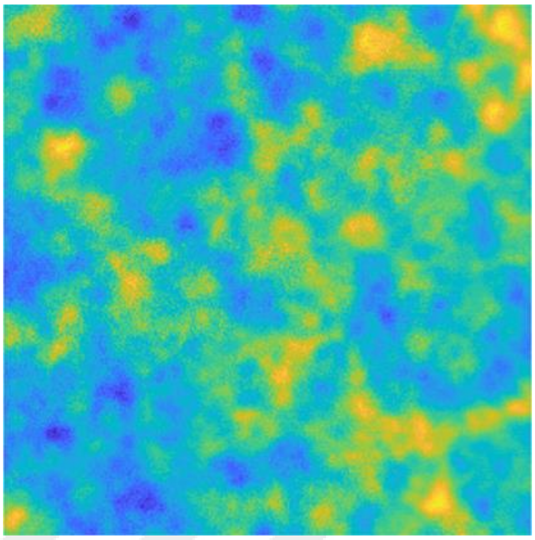

Figure 6.2. *Noisy image for 100 GHz, nd = 1, ns = 1.*

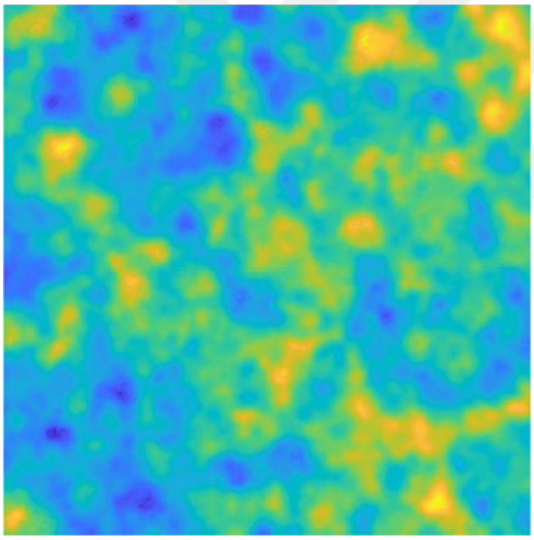

Figure 6.3. *Denoised image by our LPF- VFW for 100 GHz, nd = 1, ns = 1.*

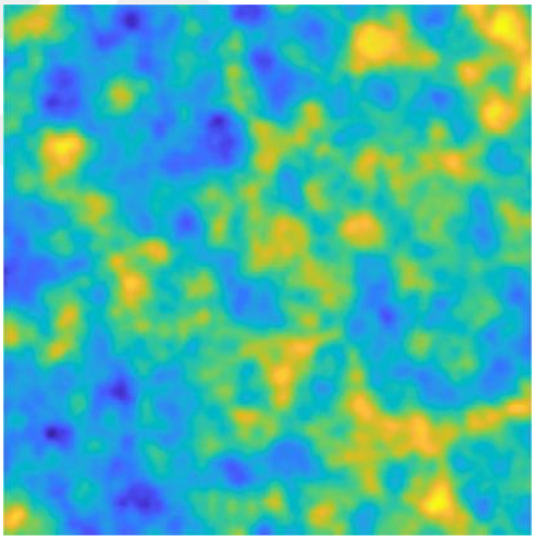

Figure 6.4. *Denoised image by the NLM + S for 100 GHz, nd = 1, ns = 1.*

Figure 6.1 and Figure 6.2 present noiseless and noisy images for 100 GHz channel, dust factor is 1 and synchrotron factor is 1. Figure 6.3 shows denoised image obtained by proposed algorithm LPF – VFW. Figure 6.4 shows the denoised image obtained by the NLM + S algorithm, which gives the best result for the image mixture with dust factor 1 and synchrotron factor 1, for the 100 GHz channel.

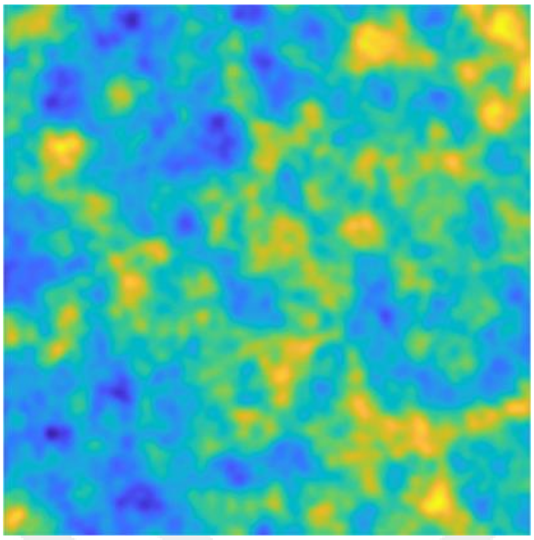

Figure 6.5. *Noiseless image for 70 GHz, nd = 1, ns = 1.*

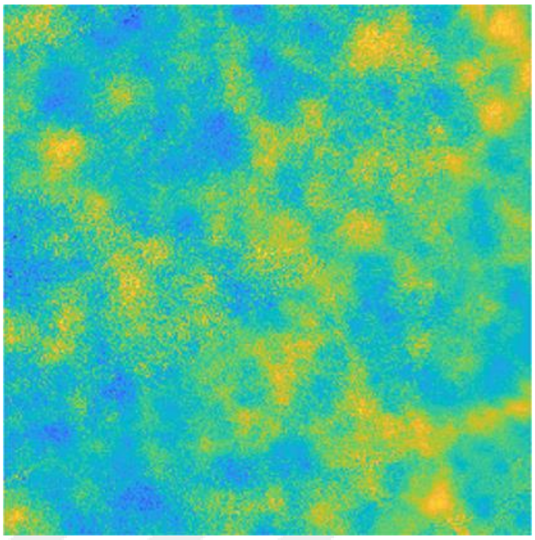

Figure 6.6. *Noisy image for 70 GHz, nd = 1, ns = 1.*

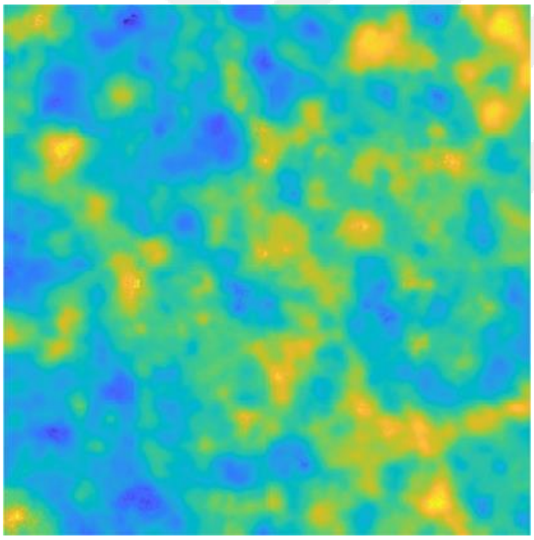

Figure 6.7. *Denoised image by our LPF - VFW for 70 GHz, nd = 1, ns = 1.*

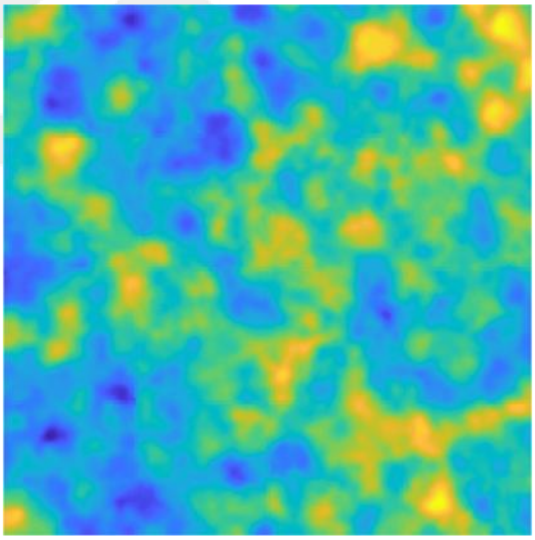

Figure 6.8. *Denoised image by the NLM + S for 70 GHz, nd = 1, ns = 1.*

Figure 6.5 and Figure 6.6 present noiseless and noisy images for 70 GHz channel, dust factor is 1 and synchrotron factor is 1. Figure 6.7 displays denoised image obtained by proposed algorithm LPF – VFW. Figure 6.8 shows the denoised image obtained by the NLM+S algorithm, which gives the best result for the image mixture with dust factor 1 and synchrotron factor 1 for the 70 GHz channel. Our algorithm is surpassed only by the NLM + S algorithm, for this mixture, among all compared methods.

7. CONCLUSION

We have proposed a vertex-frequency graph Wiener filter for denoising of graph signals defined on weighted and undirected graphs from additive, zero-mean, white noise with space varying variance. The Wiener vertex-frequency transfer function has been expressed in terms of cGRD of the original signal and its variance normalized version, assuming that the original signal is deterministic. For this deterministic noiseless signal case, we have proposed a denoising algoritm based on estimating the Wiener transfer function by using the output signal of a preliminary graph lowpass filter as the original signal estimate, and the eigenbasis of the graph Laplacian matrix obtained from the Gaussian prefiltered version of the input noisy signal as the graph basis. We have employed our proposed algorithm in denoising of astrophysical image mixtures from nonstationary instrumental noise. We have then compared our algorithm with five state of the art image denoising methods in terms of achieved PSNR figures. The proposed Wiener denoising algorithm is slightly surpassed by the NLM + S method in all mixing cases, but gives comparable results with these denoising methods. For two of the 70 GHz channel mixing cases simulating low and medium galactic contamination, our algorithm is second to the NLM + S only.

We have also developed a set of benchmarks for this denoising problem for various mixing coefficients, in Chapter 5, by using the Wiener transfer function obtained with the original, noiseless image vectors as if they are available, and graph bases similar to those of the proposed algorithm. These benchmark PSNR values are much higher than those given by all of the six compared methods. This suggests that assuming deterministic noiseless CMB, galactic dust and synchrotron components is a reasonable assumption, even though they are modeled as statistical signals in the literature [2].

REFERENCES

[1] Bluebook. The Scientific Programme of Planck, arXiv: astro-ph/0604069, 4 Apr. 2006.

[2] E. E. Kuruoglu, "Bayesian source separation for cosmology: Estimating cosmological components from multichannel measurements," *IEEE Signal Process. Mag.*, vol. 27, no. 1, pp. 43–54, Jan. 2010.

[3] M. Tegmark and G. Efstathiou, "A method for subtracting foregrounds from multifrequency CMB sky maps," *Mon. Not. Roy. Astron. Soc.*, vol. 281, no. 4, pp. 1297–1314, Aug. 1996.

[4] M. López-Caniego, D. Herranz, J. González-Nuevo, J. L. Sanz, R. B. Barreiro, P. Vielva, F. Argüeso, and L. Toffolatti, "Comparison of filters for the detection of point sources in Planck simulations," *Mon. Not. Roy. Astron. Soc., vol. 370, no. 4, pp. 2047–2063,* Aug. 2006.

[5] E. E. Kuruoğlu, L. Bedini, M. T. Paratore, E. Salerno, and A. Tonazzini, "Source separation in astrophysical maps using independent factor analysis," *Neural Networks*, vol. 16, no. 3–4, pp. 479–491, 2003.

[6] M. Costagli and E. E. Kuruoğlu, "Image separation using particle filters," *Digital Signal Process*., vol. 17, no. 5, pp. 935–946, 2007.

[7] S. P. Wilson, E. E. Kuruoğlu, and E. Salerno, "Fully Bayesian source separation of astrophysical images modelled by mixture of Gaussians," *IEEE J. Select. Top. Signal Process*., vol. 2, no. 5, pp. 685–696, Oct. 2008.

[8] A. C. Yağan and M. T. Özgen, "Spectral graph based vertex-frequency Wiener filtering for image and graph signal denoising," *IEEE Trans. Signal Inf. Process. Netw.*, vol. 6, no. 1, pp. 226–240, Dec. 2020.

[9] J.-S. Lee, "Digital image enhancement and noise filtering by use of local statistics," *IEEE Trans. Pattern Anal. Mach. Intell*., vol. PAMI-2, no. 2, pp. 165–168, Mar. 1980.

[10] D. T. Kuan, A. A. Sawchuk, T. C. Strand, and P. Chavel, "Adaptive noise smoothing filter for images with signal-dependent noise," *IEEE Trans. Pattern Anal. Mach. Intell*., vol. PAMI-7, no. 2, pp. 165-177, Mar. 1985.

[11] S.-S. Jiang and A. A. Sawchuk, "Noise updating repeated Wiener filter and other adaptive noise smoothing filters using local image statistics," *Appl. Opt*., vol. 25, no. 14, pp. 2326–2337, 1986.

[12] K. Zhang, W. Zuo, and L. Zhang, "FFDNet: Toward a fast and flexible solution for CNN-based image denoising," *IEEE Trans. Image Process*., vol. 27, no. 9, pp. 4608–4622, Sept. 2018.

[13] S. Beckouche, J. L. Starck, and J. Fadili, "Astronomical image denoising using dictionary learning," *Astron. Astrophys*., vol. 556, A132, pp. 1–14, Aug. 2013.

[14] D. I. Shuman, S. K. Narang, P. Frossard, A. Ortega, and P. Vandergheynst, ”The emerging field of signal processing on graphs: Extending high-dimensional data analysis to networks and other irregular domains,” *IEEE Signal Process. Mag.*, vol. 30, no. 3, pp. 83–98, May 2013.

[15] A. Sandryhaila and J. M. F. Moura, ”Discrete signal processing on graphs,” IEEE Trans. Signal Process., vol. 61, no. 7, pp. 1644–1656, Apr. 2013.

[16] S. Chen, A. Sandryhaila, J. M. F. Moura, and J. Kovacevic, ”Signal denoising on graphs via graph filtering,” in Proc. *IEEE Global Conf. Signal Inf. Process. (GlobalSIP)*, Dec. 2014, pp. 872–876.

[17] S. Chen, A. Sandryhaila, J. M. F. Moura, and J. Kovacevic, ”Signal recovery on graphs: Variation minimization,” *IEEE Trans. Signal Process.*, vol. 63, no. 17, pp. 4609–4624, Sep. 2015.

[18] D. K. Hammond, P. Vandergheynst, and R. Gribonval, ”Wavelets on graphs via spectral graph theory,” *Appl. Comput. Harmon. Anal.*, vol. 30, no. 2, pp. 129–150, March 2011.

[19] F. Zhang and E. R. Hancock, ”Graph spectral image smoothing using the heat kernel,” *Pattern Recognition*, vol. 41, pp. 3328–3342, Nov. 2008.

[20] E. Isufi, A. Loukas, A. Simonetto, and G. Leus, ”Autoregressive moving average graph filtering,” *IEEE Trans. Signal Process.*, vol. 65, no. 2, pp. 274–288, Jan. 15, 2017.

[21] A. Elmoataz, O. Lezoray, and S. Bougleux, ”Nonlocal discrete regularization on weighted graphs: A framework for image and manifold processing,” *IEEE Trans. Image Process.*, vol. 17, no. 7, pp. 1047–1060, Jul. 2008.

[22] A. Kheradmand and P. Milanfar, ”A general framework for kernel similarity-based image denoising,” in *Proc. IEEE Global Conf. Signal Inf. Process. (GlobalSIP)*, Dec. 2013, pp. 415–418.

[23] X. Liu, D. Zhai, D. Zhao, G. Zhai, and W. Gao, ”Progressive image denoising through hybrid graph Laplacian regularization: A unified framework,” *IEEE Trans. Image Process.*, vol. 23, no. 4, pp. 1491–1503, Apr. 2014.

[24] W. Hu, G. Cheung, X. Li, and O. C. Au, ”Graph-based joint denoising and super-resolution of generalized piecewise smooth images,” in *Proc. IEEE Int. Conf. Image Process. (ICIP)*, Paris, France, Oct. 2014, pp. 2056–2060.

[25] J. Pang and G. Cheung, ”Graph Laplacian regularization for image denoising: Analysis in the continuous domain,” *IEEE Trans. Image Process.*, vol. 26, no. 4, pp. 1770–1785, Apr. 2017.

[26] A. Gadde, S. K. Narang, and A. Ortega, ”Bilateral filter: Graph spectral interpretation and extensions,” in *Proc. IEEE Int. Conf. Image Process. (ICIP)*, Sep. 2013, pp. 1222–1226.

[27] M. Onuki and Y. Tanaka, ”Trilateral filter on graph spectral domain,” in *Proc. IEEE Int. Conf. Image Process. (ICIP)*, Paris, France, Oct. 2014, pp. 2046–2050.

[28] M. Onuki, S. Ono, M. Yamagishi, and Y. Tanaka, ”Graph signal denoising via trilateral filter on graph spectral domain,” *IEEE Trans. Signal Inf. Process. Netw*., vol. 2, no. 2, pp. 137–148, June 2016.

[29] W. Hu, X. Li, G. Cheung, and O. C. Au, ”Depth map denoising using graph-based transform and group sparsity,” in *Proc. IEEE Int. Workshop Multimedia Signal Process*., Sep. 2013, pp. 001–006.

[30] F. G. Meyer and X. Shen, ”Perturbation of the eigenvectors of the graph Laplacian: Application to image denoising,” *Appl. Comput. Harmon. Anal*., vol. 36, no. 2, pp. 326–334, Mar. 2014.

[31] Y. Iizuka and Y. Tanaka, ”Depth map denoising using collaborative graph wavelet shrinkage on connected image patches,” in *Proc. IEEE Int. Conf. Image Process. (ICIP)*, Paris, France, Oct. 2014, pp. 828–832.

[32] N. Perraudin and P. Vandergheynst, ”Stationary signal processing on graphs,” *IEEE Trans. Signal Process*., vol. 65, no. 13, pp. 3462–3477, Jul. 1, 2017.

[33] A. G. Marques, S. Segarra, G. Leus, and A. Ribeiro, ”Stationary graph processes and spectral estimation,” *IEEE Trans. Signal Process*., vol. 65, no. 22, pp. 5911–5926, Nov. 15, 2017.

[34] A. Gavili and X.-P. Zhang, ”On the shift operator, graph frequency, and optimal filtering in graph signal processing,” *IEEE Trans. Signal Process*., vol. 65, no. 23, pp. 6303–6318, Dec. 1, 2017.

[35] B. Girault, P. Gonçalves, É. Fleury, and A. S. Mor, ”Semi-supervised learning for graph to signal mapping: A graph signal Wiener filter interpretation,” in *Proc. IEEE Int. Conf. Acoust., Speech Signal Process. (ICASSP 2014)*, Mar. 2014, pp. 1115–1119.

[36] D. K. Hammond, L. Jacques, and P. Vandergheynst, ”Image denoising with non-local spectral graph wavelets,” in *Image Processing and Analysis with Graphs: Theory and Practice*. Ed. by O. Lézoray and L. Grady, CRC Press, 2012, Ch. 8, pp. 208–236.

[37] J. Irion and N. Saito, ”Efficient approximation and denoising of graph signals using the multiscale basis dictionaries,” *IEEE Trans. Signal Inf. Process. Netw*., vol. 3, no. 3, pp. 607–616, Sep. 2017.

[38] B. de Loynes, F. Navarro, and B. Olivier, ”Data-driven thresholding in denoising with spectral graph wavelet transform,” *J. Comput. Applied Math., Elsevier*, vol. 389, Article 113319, June 2021.

[39] E. Chedemail, B. de Loynes, F. Navarro, and B. Olivier, ”Large graph signal denoising with application to differential privacy,” *IEEE Trans. Signal Inf. Process. Netw*., vol. 8, pp. 788–798, 2022.

[40] A. Buades, B. Coll, and J.-M. Morel, ”A non-local algorithm for image denoising,” in Proc. *IEEE Comput. Soc. Conf. Comput. Vis. Pattern Recognit*., vol. 2, Jun. 2005, pp. 60–65.

[41] A. Buades, B. Coll, and J.-M. Morel, ”A review of image denoising algorithms, with a new one,” *SIAM J. Multiscale Modeling and Simulation: A SIAM Interdisciplinary J*., vol. 4, no. 2, pp. 490–530, 2005.

[42] C. Kervrann and J. Boulanger, ”Optimal spatial adaptation for patch-based image denoising,” *IEEE Trans. Image Process*., vol. 15, no. 10, pp. 2866–2878, Oct. 2006.

[43] P. Milanfar, ”A tour of modern image filtering: New insights and methods, both practical and theoretical,” *IEEE Signal Process*. Mag., vol. 30, no. 1, pp. 106–128, Jan. 2013.

[44] K. Dabov, A. Foi, V. Katkovnik, and K. Egiazarian, ”Image denoising by sparse 3-D transform-domain collaborative filtering,” *IEEE Trans. Image Process*., vol. 16, no. 8, pp. 2080–2095, Aug. 2007.

[45] V. Katkovnik, A. Foi, K. Egiazarian, and J. Astola, ”From local kernel to nonlocal multiple model image denoising,” *Int. J. Comput. Vis*., vol. 86, no. 1, pp. 1–32, Jan. 2010.

[46] M. T. Özgen, E. E. Kuruoğlu, and D. Herranz, ”Astrophysical image separation by blind time-frequency source separation methods,” *Digital Signal Process*., vol. 19, no. 2, pp. 360–369, March 2009.

[47] G. Cheung, E. Magli, Y. Tanaka, and M. K. Ng, “Graph spectral image processing,” *Proc. IEEE*, vol. 106, no. 5, pp. 907–930, May 2018.

[48] X. Dong, D. Thanou, L. Toni, M. Bronstein and P. Frossard, "Graph Signal Processing for Machine Learning: A Review and New Perspectives," in *IEEE Signal Processing Magazine*, vol. 37, no. 6, pp. 117-127, Nov. 2020.

APPENDIX-1

MATLAB Code for LPF-VFW

```
%Nonstationary noise with spatially varying variance, CMB+galactic dust+synchrotron mixtures
%Setting up the noiseless input image and its noisy version:
load cmb_100.dat;
load dust_100.dat;
load syn_100.dat;
load rms100.txt;
load rms70.txt;
cmb=reshape(cmb_100(:,3),256,256);
dust=reshape(dust_100(:,3),256,256);
syn=reshape(syn_100(:,3),256,256);
rms_100=reshape(rms100(:,3),256,256);
rms_70=reshape(rms70(:,3),256,256);
%CMB, dust, synchrotron, RMS map and noise images set.
X1=cmb+1000*dust+200*syn;%triple noiseless image mixture from 100GHz channel.
X2=cmb+1000*0.5085*dust+200*2.7101*syn;%triple noiseless image mixture from 70GHz channel.
%noiseless mixture images set.
alpha1=7.92/10^6/mean(rms100(:,3));
alpha2=2.19/10^5/mean(rms70(:,3));%mixture noise coefficients.
wn_100=rms_100.*randn(256,256);
wn_70=rms_70.*randn(256,256);
Y1=X1+alpha1*wn_100;
Y2=X2+alpha2*wn_70;%noisy input images.
Y=Y1(1:64,1:64);%input noisy image patch.
X=X1(1:64,1:64);%original, noiseless image patch.
[M,N]=size(Y);%input image size read.
y=Y(:);%noisy image vector.
%x=X(:);%noiseless, original image vector.
rmspatch=alpha1*rms_100(1:64,1:64);
varvec=(rmspatch(:)).^2;%true variable noise variance vector
```

```
%setting up the graph Laplacian matrix:
w=1;%window width.
Yext=zeros(M+w-1,N+w-1);%extended input image allocated.
Ky=zeros(M*N,M*N);%adjacency (or weight) matrix based on pixel values allocated.
hx=0.57;%smoothing parameter for the pixel location based weight matrix.
hy=0.017*0.000000001;%smoothing parameter for the pixel value based weight matrix.
[K,L]=meshgrid(1:M*N,1:M*N);
Mcol=ceil(K/M);
Ncol=ceil(L/M);
Mrow=rem(K,M);
Nrow=rem(L,M);
Mrow=Mrow+M*(Mrow==0);
Nrow=Nrow+M*(Nrow==0);
Kx=exp(-((Mrow-Nrow).^2+(Mcol-Ncol).^2)/hx);%adjacency (weight) matrix based on
pixel locations.
xinit=diag(1./sum(Kx.'))*Kx*y;%initial denoising by Gaussian filter.
Xinit=reshape(xinit,M,N);%initially denoised image set.
Yext((w+1)/2:M+(w-1)/2,(w+1)/2:N+(w-1)/2)=Xinit;%X;
for k=1:(w-1)/2
   Yext((w+1)/2-k,:)=Yext((w+1)/2+k,:);
   Yext(M+(w-1)/2+k,:)=Yext(M+(w-1)/2-k,:);
   Yext(:,(w+1)/2-k)=Yext(:,(w+1)/2+k);
   Yext(:,N+(w-1)/2+k)=Yext(:,N+(w-1)/2-k);
end;%extended image set, symmetrically.
for m=1:M*N
   for n=1:M*N
      Ky(m,n)=exp(-norm(Yext(Mrow(1,m):Mrow(1,m)+w-1,Mcol(1,m):Mcol(1,m) +
w-1)-Yext(Nrow(n,1):Nrow(n,1)+w-1,Ncol(n,1):Ncol(n,1)+w-1),'fro')^2/hy);
   end;
end
Lap=diag(sum(Ky.'))-Ky;%graph Laplacian matrix
[V,D]=eig(Lap);%eigendecomposition of Laplacian matrix.
yf=V.'*y;%graph FT of the input noisy image to be denoised
```

```
alpha=0.29;
xfest=(1./(1+alpha*diag(D))).*yf;%l2 regularization, graph LPF.
xest=V*xfest;%output of the graph LPF.
Xdenoised=reshape(xest,M,N);%denoised image set.
mse=mean(mean((X-Xdenoised).^2))%mse between original and denoised image.
%calculation of the cross graph Rihaczek distribution:
xfnorest=V.'*(xest./varvec);%GFT of the variance-normalized LPF output signal.
R=(xfnorest*xest.').*V.';%GRD estimate.
H=max(min(10^22,R./(V.').^2),-10^22);%unscaled Wiener transfer function estimate.
xdenoised=zeros(size(y));
for n=1:M*N
    xdenoised(n)=V(n,:)*(H(:,n).*yf);%or xfest.
end;%vertex-frequency filter applied to input image, or to the output of the graph LPF.
xdenoised=mean(y)/mean(xdenoised)*xdenoised;%scaling.
Xdenoised=reshape(xdenoised,M,N);%denoised image set.
mse=mean(mean((X-Xdenoised).^2))%mse between original and denoised image patches.

%Second step:
xdenoisedf=V.'*xdenoised;%GFT of the output of the first step.
alpha=0.15;
xdenoised=V*((1./(1+alpha*diag(D))).*xdenoisedf);%First step output passed thru a second LPF.
xfnorest=V.'*(xdenoised./varvec);
R=(xfnorest*xdenoised.').*V.';%new GRD estimate.
H=max(min(10^22,R./(V.').^2),-10^22);%new unscaled Wiener transfer function estimate.
xdenoised=zeros(size(y));
for n=1:M*N
    xdenoised(n)=V(n,:)*(H(:,n).*xdenoisedf);%or yf.
end;%vertex-frequency filter applied to input image, or to the output of the graph LPF.
xdenoised=mean(y)/mean(xdenoised)*xdenoised;%scaling.
Xdenoised=reshape(xdenoised,M,N);%denoised image set.
```

mse=mean(mean((X-Xdenoised).^2))%mse between original and denoised image patches.

CURRICULUM VITAE

ORCID ID: 0009-0005-0307-1052

Name Surname : **Sabri ÖZEN**

Foreign Language : **English**

Education and Professional Background:

- 2021 - 2024, Master’s degree in Telecommunications Program, Eskişehir Technical University, Institute of Graduate Programs, Department of Electrical and Electronics Engineering
- 2013 - 2018, Bachelor’s degree in Electrical and Electronics Engineering , Afyon Kocatepe University, Faculty of Technology